

CROWDING OUT OF GIANTS BY DWARFS: AN ORIGIN FOR THE LACK OF COMPANION PLANETS IN HOT JUPITER SYSTEMS

MASAHIRO OGIHARA

Nagoya University, Furo-cho, Chikusa-ku, Nagoya, Aichi 464-8602, Japan

SHU-ICHIRO INUTSUKA

Nagoya University, Furo-cho, Chikusa-ku, Nagoya, Aichi 464-8602, Japan

AND

HIROSHI KOBAYASHI

Nagoya University, Furo-cho, Chikusa-ku, Nagoya, Aichi 464-8602, Japan

Draft version August 16, 2018

ABSTRACT

We investigate formation of close-in terrestrial planets from planetary embryos under the influence of a hot Jupiter (HJ) using gravitational N -body simulations that include gravitational interactions between the gas disk and the terrestrial planet (e.g., type I migration). Our simulations show that several terrestrial planets efficiently form outside the orbit of the HJ, making a chain of planets, and all of them gravitationally interact directly or indirectly with the HJ through resonance, which leads to inward migration of the HJ. We call this mechanism of induced migration of the HJ as “crowding out.” The HJ is eventually lost by collision with the central star, and only several terrestrial planets remain. We also find that the efficiency of the crowding-out effect depends on model parameters; for example, the heavier the disk is, the more efficient the crowding out is. When planet formation occurs in a massive disk, the HJ can be lost to the central star and is never observed. On the other hand, for a less massive disk, the HJ and terrestrial planets can coexist; however, the companion planets can be below the detection limit of current observations. In both cases, systems with the HJ and terrestrial planets have little chance for detection. Therefore, our model naturally explains the lack of companion planets in HJ systems regardless of the disk mass. In effect, our model provide a theoretical prediction for future observations; additional planets can be discovered just outside the HJ, and their masses should generally be small.

Subject headings: planets and satellites: formation – planets and satellites: terrestrial planets – planet-disk interactions

1. INTRODUCTION

Recent observations have found multiple-planet systems whose architectures differ strikingly from that of our solar system. One of the most distinctive features is a lack of companion planets in HJ systems (e.g., Latham et al. 2011; Steffen et al. 2012). Although some exceptions are being brought out by the *Kepler* survey, this trend is clearly seen in recent observational results. Several ideas for the inhibition of planet formation in the vicinity of HJs were presented (Fogg & Nelson 2007; Raymond et al. 2011). We propose a new way of explaining this observational property.

The combination of radial velocity and transit detection observations provides information on the average densities of planets (e.g., Borucki et al. 2010), which shows that a significant fraction of HJs are gaseous giant planets. This clearly means that HJs are surrounded by gaseous components in protoplanetary disks, at least during their formation stages. A natural question in this regard is what happened in the protoplanetary disks in the presence of HJs. It might be interesting to theoretically probe the condition of planet formation in the presence gaseous giants.

We investigate the formation of terrestrial planets in

the presence of an HJ. For the origin of HJs, although type II migration (e.g., Lin et al. 1996) and tidal circularization of high-eccentricity planets (e.g., Ford & Rasio 2006; Nagasawa et al. 2008) were proposed, we here introduce a hybrid scenario in which HJs can be formed through gravitational instability prior to growth of terrestrial planets (Inutsuka 2009). Recent progress in our understanding of protostar formation provides an explanation regarding the formation of protoplanetary disks and their accretion onto the central protostar in their early evolutionary phases (see review by Inutsuka (2012)). One of the findings from high-resolution numerical simulations that describe the gravitational collapse of molecular cloud cores indicates that new-born protoplanetary disks are gravitationally unstable and produce multiple planetary mass objects that tend to chaotically migrate in the massive disks (Vorobyov & Basu 2010; Machida et al. 2011). Although the final fates of those planetary mass objects are not entirely clear, the objects that were formed relatively late may survive and remain as gaseous giants in various locations in the disks. Therefore it is natural to consider the planet formation process under the influence of gaseous giants in protoplanetary disks.

The letter proceeds as follows. In Section 2, we describe our numerical model; in Section 3, we present the

results of simulations. In Section 4, we derive the condition for migration of HJ. In Section 5, we present a discussion.

2. MODEL DESCRIPTION

An HJ with Jovian mass is initially placed at $a_{\text{HJ}} = 0.05\text{AU}$ on a circular orbit, where a_{HJ} is the semimajor axis of the HJ. Under the influence of the HJ, formation of solid planets from planetary embryos are investigated using numerical simulations that combine the N -body code and the semianalytical code.

The simulation domain of N -body calculations is set between 0.02 and 0.5 AU and the gravitational forces between all the bodies are calculated (in the same manner as in previous works by Ogihara et al. 2007; Ogihara & Ida 2009, 2012). For the initial solid disk, the solid surface density is assumed as

$$\Sigma_{\text{d}} = 10f_{\text{d}} \left(\frac{r}{1 \text{ AU}} \right)^{-3/2} \text{ g cm}^{-2}, \quad (1)$$

where f_{d} is a scaling factor and r is the radial distance from the central star. According to this density distribution, planetary embryos are placed with the isolation mass of $M_{\text{iso}} = 2\pi a \Delta a \Sigma_{\text{d}}$, where Δa is the width of the feeding zone and assumed to be $\simeq 10$ Hill radii. Note that protoplanets reach the isolation masses for the parameters we are concerned with, unless significant loss of surface density caused by collisional fragmentation occurs (Kobayashi et al. 2010).

The effect of type I migration is considered; thus, protoplanets migrate in to the simulation domain from beyond 0.5 AU. We also simulate the growth and migration of protoplanets beyond 0.5 AU not by N -body code but by semianalytical code in the same manner as in the population synthesis model (e.g., Ida & Lin 2008), where protoplanets migrate after their growing. When protoplanets reach the boundary ($a = 0.5\text{AU}$), the bodies are added to the N -body code.

We incorporate the effects of eccentricity and inclination damping and orbital migration due to gravitational interaction with the gas disk (e.g., Ogihara & Ida 2009; Ogihara et al. 2010). The decay rate of semimajor axis is (Tanaka et al. 2002)

$$\begin{aligned} t_a &= \frac{1}{C_1} \frac{1}{2.7 + 1.1q(r)} \left(\frac{M}{M_*} \right)^{-1} \left(\frac{\Sigma_{\text{g}} r^2}{M_*} \right)^{-1} \left(\frac{c_{\text{s}}}{v_{\text{K}}} \right)^2 \Omega^{-1} \\ &= 1.6 \times 10^3 C_1^{-1} f_{\text{g}}^{-1} \left(\frac{2.7 + 1.1q(r)}{4.35} \right)^{-1} \left(\frac{r}{0.1 \text{ AU}} \right)^{3/2} \\ &\quad \times \left(\frac{M}{M_{\oplus}} \right)^{-1} \left(\frac{M_*}{M_{\odot}} \right)^{-1/2} \left(\frac{L_*}{L_{\odot}} \right)^{1/4} \text{ yr}, \end{aligned} \quad (3)$$

where C_1 and $-q(r)$ denote the type I migration efficiency factor (Ida & Lin 2008) and the gas surface density gradient ($q(r) = -d \ln \Sigma_{\text{g}} / d \ln r$), respectively.¹ The migration can be halted when the planets are captured in a mean motion resonance with the HJ (e.g., Ogihara & Kobayashi 2013) or they reach a region with

¹ Note that the direction and rate of the type I migration can be altered in a non-isothermal disk; several factors that depend on the local gradient of temperature and entropy should be added to the above equations (e.g., Paardekooper et al. 2010).

positive density gradient. The latter corresponds to locations on the disk inner edge (e.g., magnetospheric cavity) or the outer edge of a gap that is opened by the HJ; terrestrial planets in these locations can gain a positive torque from the disk by the steep surface density gradient (Masset et al. 2006). Planets stop their migration at density gaps or resonance locations, whichever are first encountered by the planets (i.e., whichever is at the more distant location from the star).

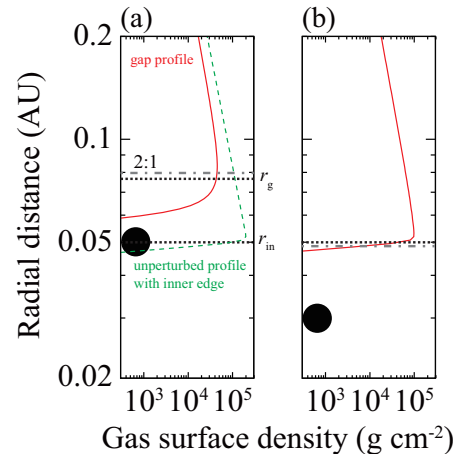


FIG. 1.— The dashed line represents the unperturbed disk profile for $f_{\text{g}} = 1$ with the inner edge, where the gas density smoothly vanishes at 0.05 AU with the width of the disk scale height. (a) The solid line shows the disk profile, in which a density gap is opened by the HJ at 0.05 AU. The dotted lines indicate the location of $q(r) = -2.7/1.1$ for this gap profile, which exist inside the 2:1 resonance with the HJ (dot-dashed line). (b) The disk profile for the HJ at 0.03 AU.

The unperturbed gas surface density is considered to be of the form

$$\Sigma_{\text{g}} = 2400f_{\text{g}} \left(\frac{r}{1 \text{ AU}} \right)^{-3/2} \exp \left(\frac{-t}{t_{\text{dep}}} \right) \text{ g cm}^{-2}, \quad (4)$$

where f_{g} is a scaling factor (Hayashi 1981). We usually assume $f_{\text{g}} = 1$ in our simulations. For the case of $f_{\text{d}}/f_{\text{g}} = 1$, the solar metallicity is considered. Note that there is a vast range in the metallicity of stars; we vary the values of f_{d} and/or f_{g} in order to change the metallicity. The gas disk exponentially dissipates on the depletion timescale of $t_{\text{dep}} = 10^6 \text{ yr} \simeq 3 \times 10^7 T_{\text{K}}$, where T_{K} is the orbital period at 0.1 AU. The unperturbed gas surface density profile is shown by the dashed line in Figure 1(a). We consider a disk inner edge, r_{in} , at 0.05 AU from the central star and inside of which there is a cavity. The HJ opens up a gap near its orbit; for gap profile computations we use an analytical description developed by Crida et al. (2006), which depends on the disk viscosity. In this study, relatively high value for the turbulent viscosity is assumed ($\alpha = 10^{-2}$), where α denotes the disk viscosity. We will discuss the dependence of the disk viscosity in the following paper (Ogihara et al., in prep.). The gas surface density profile, which includes the density gap, is shown by the solid line in Figure 1(a). At the gap edge, $q(r)$ becomes smaller than $-2.7/1.1$, which cause a positive torque on the planet. The location of $q(r) = -2.7/1.1$ for the gap edge r_{g} is shown by the dotted line in Figure 1. The location of the 2:1

resonance with the HJ is shown by the dot-dashed line, which is further from the central star than the gap assuming $a_{\text{HJ}} = 0.05\text{AU}$. When the HJ comes very close to the central star ($\lesssim 0.03\text{AU}$), the locations of the 2:1 resonance and the gap edge move inside r_{in} (Figure 1(b)).

If HJs move to very close-in orbits, the tidal interaction with the star would be important. The migration timescale induced by the tidal torque is (Goldreich & Soter 1966)

$$t_{a,\text{tide}} = \left| \frac{a}{\dot{a}} \right| = \frac{Q_*}{3k_{2,*}} \left(\frac{M}{M_*} \right)^{-1} \left(\frac{a}{R_*} \right)^5 \Omega^{-1}, \quad (5)$$

where Q_* and $k_{2,*}$ are the tidal dissipation function and the love number of the central star, respectively. Assuming $M_* = M_\odot$ and $R_* = R_\odot$, the timescale is reduced to

$$t_{a,\text{tide}} = 6 \times 10^9 \left(\frac{Q_*}{10^6} \right) \left(\frac{k_{2,*}}{0.3} \right)^{-1} \left(\frac{M_{\text{HJ}}}{M_{\text{J}}} \right)^{-1} \left(\frac{a}{0.03\text{AU}} \right)^{6.5} \quad (6)$$

which is a strong function of a . We also incorporate this damping in our simulations, adopting a slightly smaller value of $Q_* = 10^5$ to reduce the computational cost, which does not change our conclusions for $Q_* \lesssim 10^6$. Note that if HJs reach 0.02 AU, they can fall onto the star within several 10^8 yr even assuming conservative values of $Q_* = 10^6$ and $R_* = R_\odot$. Thus, we set the inner boundary of the computational region at 0.02 AU.

3. RESULTS

In Figure 2(a), we show the time evolution of semimajor axis for our fiducial model parameters, where $f_d = f_g = C_1 = 1$ is assumed. The time unit is expressed by the orbital period at 0.1 AU (lower axis) and by yr (upper axis). All bodies are plotted as filled circles connected with solid lines, whereas the HJ is represented by open circles. The dotted line represents the location of $q(r) = -2.7/1.1$; the inner disk profile is determined by the gap opened by the HJ ($t \lesssim 9 \times 10^7 T_K$), whereas it is determined by the inner cavity in the late stage of the simulation. Planetary embryos that are initially placed inside 0.5 AU undergo inward migration. The innermost planet stops its migration when it is captured into the 2:1 mean motion resonance with the HJ at $t \simeq 2 \times 10^5 T_K$. Other migrating protoplanets approach the inner planet, which is captured in the 2:1 resonance, and interact with each other, leading to mergers or captures into mean motion resonances. As a result, several planets relax to a quasi-steady state captured in mutual mean motion resonances, which is called a chain of resonant planets or a “resonant chain.”

After that, several planetary embryos whose growth is calculated using the semianalytical code migrate inward from outside 0.5 AU.² These protoplanets also interact with the planets in the resonant chain, and eventually participate in the resonant chain. Because the innermost planet is located outside the gap edge, the planets in the

² We see an unphysical time gap between 10^6 and $10^7 T_K$, which can be attributed to the fact that the growth of protoplanets inside 0.5 AU is not simulated in this work. Note, however, that this produces no systematic change in the final state of planetary architecture, which is confirmed by high-resolution simulations (Ogihara et al., in prep.).

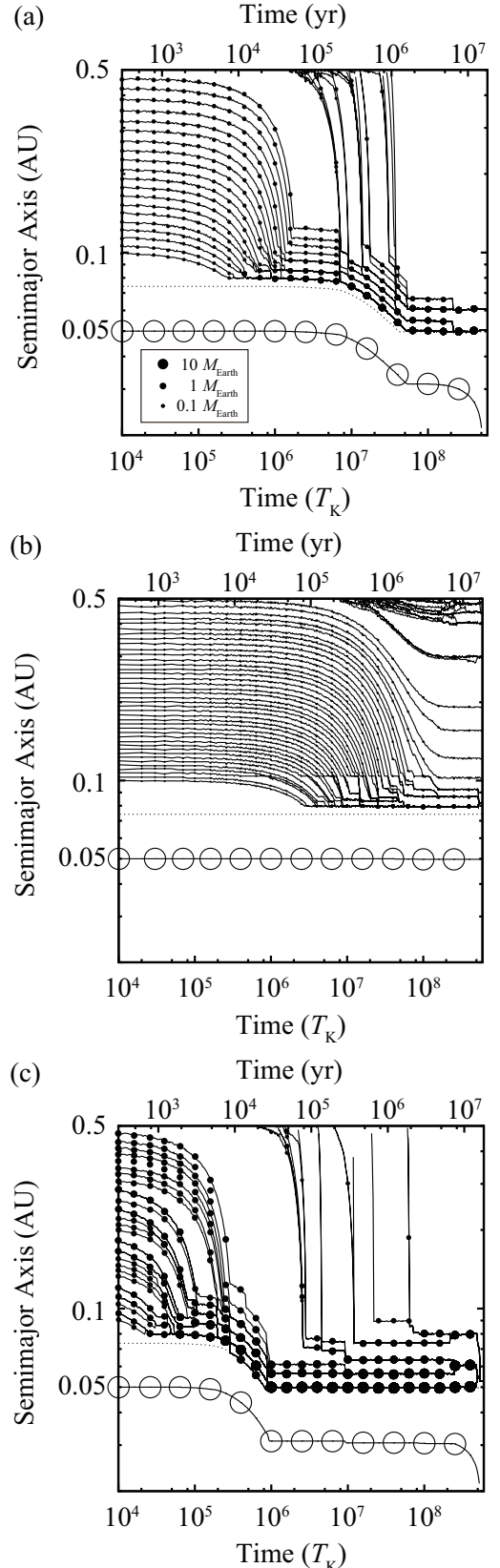


FIG. 2.— Evolution of systems for (a) the fiducial model, (b) the decreased solid surface density ($f_d = 0.1$), and (c) the increased solid surface density ($f_d = 10$). The open circles connected with solid lines represent the HJ, whereas the solid circles show the evolution of other bodies. The dotted lines indicate the location of $q(r) = -2.7/1.1$ in the gas disk.

resonant chain reside in the region of negative density gradient in the gas disk and keep losing the orbital angular momentum by the negative type I migration torque. Through gravitational interaction between the HJ and the planets in the resonant chain, the HJ migrate inward by being pushed in by the resonant chain as a whole, although the HJ itself is in the cavity of the gas disk. We call this phenomenon a “crowding out” effect. Note that the crowding out may also occur due to the interaction between an HJ and a massive swarm of planetesimals feeling strong aerodynamical gas drag (Raymond et al. 2006; Mandell et al. 2007).

When the HJ comes to a very close-in orbit ($a \simeq 0.03\text{AU}$), the location of the 2:1 resonance with the HJ is comparable to the location of the disk inner edge at 0.05 AU (Figure 1(b)). The innermost planet in the resonant chain reaches the disk inner edge and gains the positive torque from the disk, which compensates for the net negative torque exerted on the planets in the resonant chain; the inward migration of the HJ due to the crowding-out effect is halted at $t \simeq 9 \times 10^7 T_K$.³

The disk gas is depleted on the timescale of $10^6\text{yr} \simeq 3 \times 10^7 T_K$. Then, only the HJ moves inward because of the tidal torque from the host star, which results in widening separation between the HJ and the innermost planet. This leads to a deviation from the 2:1 resonance, and subsequently some planets exhibit orbit crossing. In this run, two giant impact events between planets are observed at $t \simeq 2.1 \times 10^8 T_K$, which results in losses of commensurate relationships. The HJ is lost to the central star⁴, and two terrestrial planets remain at the end of simulation. The largest planet has $M = 2.3M_\oplus$.

Figures 2(b) and (c) show the results with decreased ($f_d = 0.1$) and increased ($f_d = 10$) solid surface density, respectively. Although the HJ gravitationally interacts with the resonant chain, the inward migration of the HJ caused by the crowding out is not seen in the result of decreased solid density ($f_d = 0.1$) because small planets formed in the less massive disk, feeling weak type I migration torques, cannot effectively reduce the angular momentum of the HJ through resonant interactions. The largest planet has a mass of $0.15M_\oplus$ at the end of simulation. The migration of the HJ due to the tidal torque from the star is also not observed because the HJ has a larger semimajor axis ($a \simeq 0.05\text{AU}$). Several planets have commensurate relations in the final state. On the other hand, the crowding out of the HJ is clearly observed in the result of increased density ($f_d = 10$). In fact, the timescale of inward migration of the HJ is shortened. Relatively large planets with maximum mass of $24M_\oplus$ remain in the final state.

4. CONDITION FOR CROWDING OUT OF HJ

We now derive the condition for inward migration of the HJ due to the crowding out within the disk lifetime. When the HJ moves close to the central star, it can subsequently be lost to the star because of the tidal evolution. Therefore, the condition for crowding out can simply correspond to the condition for the loss of HJ.

³ Note that if r_{in} is closer to the star than that assumed in this letter, the HJ migrates inside 0.03 AU due to the crowding out.

⁴ The HJ at 0.03 AU can fall onto the star within a few billion years for $Q_* < 10^6$.

The timescale of the HJ’s induced migration due to the crowding-out effect, $t_{a,\text{HJ}}$, which depends on the total mass in planets in the resonant chain (M_{chain}) and on the migration timescale of planets in the chain ($t_{a,\text{chain}}$), is given by

$$t_{a,\text{HJ}} = -\frac{J_{\text{HJ}}}{2T_{\text{chain}}} \simeq t_{a,\text{chain}} \left(\frac{a_{\text{HJ}}}{a_{\text{chain}}} \right)^{1/2} \frac{M_{\text{HJ}}}{M_{\text{chain}}}, \quad (7)$$

where J_{HJ} and T_{chain} are, respectively, the angular momentum of the HJ and the total migration torque exerted on the planets in the resonant chain. a_{chain} and $t_{a,\text{chain}}$ are the typical values for the semimajor axis and the migration timescale of the planets in the resonant chain.

Assuming that all the bodies that migrate to near 0.1 AU are included in the resonant chain, we derive the total mass of the migrating planets M_{chain} . Because the type I migration speed increases with increasing mass, bodies grow to a certain mass and then start migration. The mass of migrating planets is expressed by the critical mass for migration, which is determined by a balance between the accretion timescale and the migration timescale, or the isolation mass, whichever is smaller. The isolation mass is smaller in the inner region; thus, we can define a boundary a_{trans} , inside which all the migrating planets are with the isolation mass.

The total mass of the migrating planets is given by

$$M_{\text{chain}} \simeq \int_{a_{\text{in}}}^{a_{\text{max}}} \Sigma_{\text{d}} 2\pi r dr, \quad (8)$$

where a_{in} is the radius of the inner edge of the initial solid disk, and a_{max} denotes the maximum semimajor axis, inside which solid bodies can start migration before the disk gas is depleted. We assume $a_{\text{in}} = 0$ for simplicity. When input parameters (f_d , C_1 , and f_g) are specified, a unique value for a_{max} is determined.

We first consider the case where planets with the isolation mass can only migrate inward; the condition for $a_{\text{trans}} > a_{\text{max}}$ is given by

$$2 \left(\frac{t_{\text{dep}}}{10^6\text{yr}} \right)^{4/3} f_d^{27/11} C_1^{59/33} f_g^{53/33} \lesssim 1, \quad (9)$$

where $M_* = M_\odot$ and $L_* = L_\odot$ are assumed hereafter. Then the maximum semimajor axis a_{max} is deduced by equating the migration timescale $t_a|_{M=M_{\text{iso}}}$ with the disk depletion timescale t_{dep} . Substituting a_{max} into Equation (8), we obtain

$$M_{\text{chain,iso}} \simeq 0.1 \left(\frac{t_{\text{dep}}}{10^6\text{yr}} \right)^{2/3} \left(\frac{f_d}{0.1} \right)^3 C_1^{2/3} f_g^{2/3} M_\oplus \quad (10)$$

Note that this should be overestimated by about a factor of 2–5 because the integral in Equation (8) is performed from the central star for simplicity. Then the migration timescale of the HJ is approximated by

$$t_{a,\text{HJ,iso}} \simeq 4 \times 10^7 \zeta^{-1} \left(\frac{a_{\text{HJ}}}{0.05\text{AU}} \right)^{1/2} \left(\frac{M_{\text{HJ}}}{M_J} \right) \left(\frac{t_{\text{dep}}}{10^6\text{yr}} \right)^{-4/3} \times \left(\frac{f_d}{0.1} \right)^{-4} C_1^{-7/3} f_g^{-7/3} \left(\frac{a_{\text{chain}}}{0.1\text{AU}} \right) \text{yr}, \quad (11)$$

where a correction factor ζ is introduced. In addition to the overestimate of M_{chain} , the gas density profile also

accounts for this correction. Although we adopt Equation (4) and derive the migration timescale, both Σ_g and $q(r)$ become smaller around $r = 0.1\text{AU}$. We put all of these corrections into the factor ζ .

When the planets migrate inward from the outer region where the mass is determined by the critical mass for migration ($a_{\text{trans}} < a_{\text{max}}$), the total mass in the resonant chain is estimated by

$$M_{\text{chain,crit}} \simeq 5.6 \left(\frac{t_{\text{dep}}}{10^6 \text{yr}} \right)^{5/24} f_d^{37/32} C_I^{5/96} f_g^{11/96} M_{\oplus} \quad (12)$$

Note again that this is somewhat overestimated. The migration timescale of the HJ is given by

$$t_{a,\text{HJ,crit}} \simeq 1 \times 10^4 \zeta^{-1} \left(\frac{a_{\text{HJ}}}{0.05 \text{AU}} \right)^{1/2} \left(\frac{M_{\text{HJ}}}{M_J} \right) \left(\frac{t_{\text{dep}}}{10^6 \text{yr}} \right)^{-5/12} \times f_d^{-37/16} C_I^{-53/48} f_g^{-59/48} \left(\frac{a_{\text{chain}}}{0.1 \text{AU}} \right) \text{yr}, \quad (13)$$

where ζ is the correction factor as mentioned above. By comparing this expression with the actual migration timescale observed in simulations, we find $\zeta \simeq 0.01$.

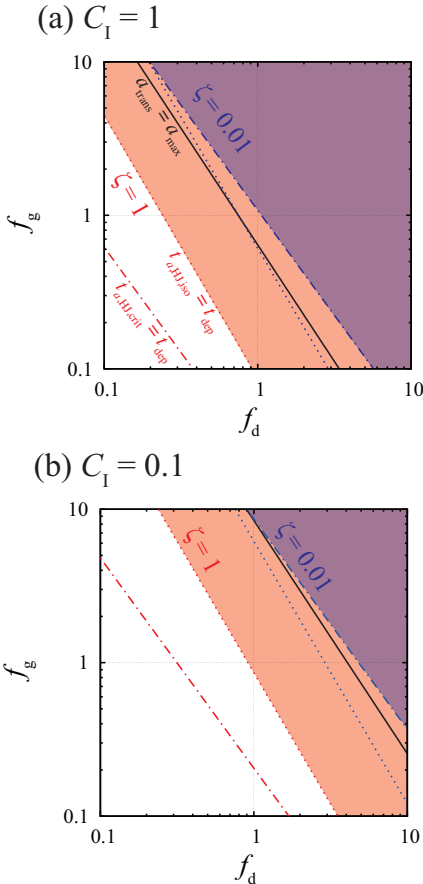


FIG. 3.— The migration timescale of the HJ ($t_{a,\text{HJ}}$) is compared with the disk depletion timescale (t_{dep}). The solid, dotted, and dash-dotted lines indicate $a_{\text{trans}} = a_{\text{max}}$, $t_{a,\text{HJ,iso}} = t_{\text{dep}}$, and $t_{a,\text{HJ,crit}} = t_{\text{dep}}$, respectively. The regions where the crowding out occurs are hatched; the gray-hatched (red in the online journal), and the dark-hatched (blue in the online journal) regions show the conditions for $\zeta = 1$ and $\zeta = 0.01$, respectively. (a) The case of $C_I = 1$. (b) The case of $C_I = 0.1$.

In Figure 3, we plot the condition for migration ($t_{a,\text{HJ}} < t_{\text{dep}}$) due to the crowding out on the $f_d - f_g$ plane for $\zeta = 1$ (gray-hatched region) and 0.01 (dark-hatched region). Figure 3(a) is the case where the full type I migration rate is considered ($C_I = 1$), whereas Figure 3(b) shows the condition for $C_I = 0.1$. We find that the parametric region in which the crowding out is effective is not so limited; in fact, the effect becomes rather common when the gas or solid surface densities are larger than the minimum mass solar nebular model ($f_g f_d > 1$). The condition for crowding out is not expected to depend on the metallicity (f_d/f_g). There is a correlation between the stellar metallicity and the probability of an HJ (e.g., Fischer & Valenti 2005), which can be explained if HJs are more likely to form around high-metallicity stars.

5. POSSIBLE EXPLANATION FOR PROPERTY OF CLOSE-IN EXOPLANETS

The origin of the lack of companion planets close to HJs can be naturally explained using our model. When the crowding out of HJ is effective (e.g., the disk mass ($f_d f_g$) is large), the HJ can be pushed inward by a chain of resonant planets, leading to a collision with the central star. Therefore, the HJ is never observed, whereas other terrestrial planets remain around 0.1 AU. On the other hand, when the crowding out is not effective (e.g., in a low-mass disk), the HJ and companion planets may coexist. However, their masses and/or sizes are below the detection limit of the current survey. In both cases, systems with the HJ and close-in terrestrial planets have little chance to be detected.

Our model provides a theoretical prediction for future observations. That is, if additional planets will be found just outside the HJ, the masses of planets are likely to be small. In those systems, the maximum mass for solid planets can be estimated by equating $t_{a,\text{HJ}}$ and t_{dep} as

$$M_{\text{chain,max}} \simeq 0.6 \zeta^{-1/2} \left(\frac{a_{\text{HJ}}}{0.05 \text{AU}} \right)^{1/4} \left(\frac{M_{\text{HJ}}}{M_J} \right)^{1/2} \left(\frac{t_{\text{dep}}}{10^6 \text{yr}} \right)^{-1/2} \times C_I^{-1/2} f_g^{-1/2} \left(\frac{a_{\text{chain}}}{0.1 \text{AU}} \right)^{1/2} M_{\oplus}. \quad (14)$$

In addition, if many exoplanets that contradict our prediction are detected, it means that some of the assumptions made in our model should be invalid. One possibility is that the inner edge of the gaseous disk is much larger than our choice at the formation stage of terrestrial planets, which makes the crowding out inefficient. Whatever observational results we obtain, the implications of our results may impose some constraints on the planet formation theory.

ACKNOWLEDGMENT

We thank the anonymous referee for useful comments. We also thank Shoichi Oshino, Eiichiro Kokubo, and Yasunori Hori for fruitful discussions. Numerical computations were in part conducted on the general-purpose PC farm at CfCA of NAOJ.

REFERENCES

- Borucki, W. J. 2010, *Science*, 327, 977
- Crida, A., Morbidelli, A., & Masset, F. 2006, *Icarus*, 181, 587
- Fischer, D. A., & Valenti, J. 2005, *ApJ*, 622, 1102
- Fogg, M. J., & Nelson, R. P. 2007, *A&A*, 472, 1003
- Ford, E. B., & Rasio, F. A. 2006, *ApJ*, 638, L45
- Goldreich, P., & Soter, S. 1966, *Icarus*, 5, 375
- Hayashi, C. 1981, *Prog. Theor. Phys. Suppl.*, 70, 35
- Ida, S. & Lin, D. N. C. 2008, *ApJ*, 673, 484
- Inutsuka, S. 2009, in *Proc. EXOPLANETS AND DISKS: THEIR FORMATION AND DIVERSITY*, ed. T. Usuda, M. Tamura, & M. Ishii (Melville, NY: AIP), 1158, 31
- Inutsuka, S. 2012, *Prog. Theor. Exp. Phys.*, 01A307
- Kobayashi, H., Tanaka, H., Krivov, A. V., & Inaba, S. 2010, *Icarus*, 209, 836
- Latham, D. W. et al. 2011, *ApJ*, 732, L24
- Lin, D. N. C., Bodenheimer, P., & Richardson, D. C. 1996, *Nature*, 380, 606
- Machida, M. N., Inutsuka, S., & Matsumoto, T. 2011, *ApJ*, 729, 42
- Mandell, A. M., Raymond, S. N., & Sigurdsson, S. 2007 *ApJ*, 660, 823
- Masset, F. S., D'Angelo, G., & Kley, W. 2006, *ApJ*, 652, 730
- Nagasawa, M., Ida, S., & Bessho, T. 2008, *ApJ*, 678, 498
- Ogihara, M., & Ida, S. 2009, *ApJ*, 699, 824
- Ogihara, M., & Ida, S. 2012, *ApJ*, 753, 60
- Ogihara, M., & Kobayashi, H. 2013, *ApJ*, 775, 34
- Ogihara, M., Ida, S. & Morbidelli, A. 2007, *Icarus*, 188, 522
- Ogihara, M., Duncan, M. J., & Ida, S. 2010, *ApJ*, 721, 1184
- Paardekooper, S.-J., Baruteau, C., Crida, A., & Kley, W. 2010, *MNRAS*, 401, 1950
- Raymond, S. N., Mandell, A. M., & Sigurdsson, S. 2006, *Science*, 313, 1413
- Raymond, S. N., Armitage, P. J., Moro-Martín, A., Booth, M., Wyatt, M. C., Armstrong, J. C., Mandell, A. M., Selsis, F., & West, A. A. 2011, *A&A*, 530, A62
- Steffen, J. H. et al. 2012, *PNAS*, 109, 7982
- Tanaka, H., Takeuchi, T., & Ward, W. R. 2002, *ApJ*, 565, 1257
- Vorobyov, E. I., & Basu, S. 2010, *ApJ*, 714, L133